**Review Article**

Kunrada Kankam, Watcharaporn Cholamjiak, and Prasit Cholamjiak*

# New inertial forward–backward algorithm for convex minimization with applications

https://doi.org/10.1515/dema-2022-0188
received July 22, 2022; accepted November 27, 2022

**Abstract:** In this work, we present a new proximal gradient algorithm based on Tseng's extragradient method and an inertial technique to solve the convex minimization problem in real Hilbert spaces. Using the stepsize rules, the selection of the Lipschitz constant of the gradient of functions is avoided. We then prove the weak convergence theorem and present the numerical experiments for image recovery. The comparative results show that the proposed algorithm has better efficiency than other methods.

**Keywords:** Tseng's extragradient method, image recovery, inertial technique, minimization problem

**MSC 2020:** 65K05, 90C25, 90C30

## 1 Introduction and preliminaries

The forward–backward splitting (FBS) algorithm [1,2] was proposed for solving the convex minimization problem (MNP) of two objective functions in a real Hilbert space $H$. It is modeled as the following form:

$$\min\{f(k) + g(k) : k \in H\}, \tag{1.1}$$

where $f : H \to (-\infty, +\infty]$ and $g : H \to \mathbb{R}$ are two proper lower semicontinuous convex functions such that $f$ is differentiable on $H$. The FBS generates an iterative sequence $k^0 \in H$ and

$$k^{n+1} = \underbrace{\mathrm{prox}_{\lambda_n g}}_{\text{backward step}} \underbrace{(k^n - \lambda_n \nabla f(k^n))}_{\text{forward step}}, \tag{1.2}$$

where $\lambda_n > 0$, $\mathrm{prox}_{\lambda_n g} = (I + \lambda_n \partial g)^{-1}$ is the proximal operator of $g$, and $\nabla f$ is the gradient of $f$. The proximal operator is single-valued with full domain, and it is characterized by the relations

$$\frac{k - \mathrm{prox}_{\lambda g}(k)}{\lambda} \in \partial g(\mathrm{prox}_{\lambda g}(k)), \tag{1.3}$$

for all $k \in H$ and $\lambda > 0$. The subdifferential of $g$ is the set-valued operator $\partial g : H \to 2^H$, which is defined by

$$\partial g(k) = \{u \in H | g(x) - g(k) \ge \langle u, x - k \rangle, x \in H\}.$$

The elements in $\partial g(k)$ are called the subgradient of $g$ at $k$. The FBS includes, as a special case, the proximal point algorithm [3–9] and the gradient method [10–12]. Due to its wide applications, there have been modifications of (1.2) invented in the literature [13–16].

*** Corresponding author: Prasit Cholamjiak,** School of Science, University of Phayao, Phayao 56000, Thailand, e-mail: prasitch2008@yahoo.com
**Kunrada Kankam:** School of Science, University of Phayao, Phayao 56000, Thailand, e-mail: kunradazzz@gmail.com
**Watcharaporn Cholamjiak:** School of Science, University of Phayao, Phayao 56000, Thailand, e-mail: c-wchp007@hotmail.com

In 2000, Tseng [17] introduced the forward–backward-forward splitting (FBFS) algorithm, also known as Tseng's extragradient algorithm or Tseng's method. FBFS is generated by $k^0 \in H$ and

$$k^{n+1} = \mathrm{prox}_{\alpha_n g}(k^n - \alpha_n \nabla f(k^n)) - \alpha_n\Big(\nabla f\Big(\mathrm{prox}_{\alpha_n g}(k^n - \alpha_n \nabla f(k^n))\Big) - \nabla f(k^n)\Big),$$

where $(\alpha_n)$ is a real positive sequence. In 2005, Combettes and Wajs [1] proposed the relaxed version of FBS (FBS-CW), which is generated by $k^0 = k^1 \in H$, $\varepsilon \in (0, \min\{1, 1/L\})$, and

$$k^{n+1} = k^n + \lambda_n(\mathrm{prox}_{\alpha g}(k^n - \alpha_n \nabla f(k^n)) - k^n), \tag{1.4}$$

where $\lambda_n \in [\varepsilon, 1]$, $\alpha_n \in [\varepsilon, (2/L) - \varepsilon]$, and $L$ is the Lipschitz constant of $\nabla f$.

To improve the convergence of the algorithm, a popular technique is using inertial-type methods. For other inertial methods, we refer to [18–23]. In this work, we consider the inertial forward–backward method [18,24] (IFB), which is generated by $k^0 = k^1 \in H$ and

$$x^n = k^n + \theta_n(k^n - k^{n-1}), \quad k^{n+1} = \mathrm{prox}_{\alpha_n g}(x^n - \alpha_n \nabla f(x^n)), \tag{1.5}$$

where $(\alpha_n)$ is a real positive sequence, $\theta_n > 0$. Here, $\theta_n$ is an extrapolation factor, and the inertial is represented by the term $\theta_n(k^n - k^{n-1})$. In 2009, Beck and Teboulle [24] introduced a fast iterative shrinkage-thresholding algorithm method (FISTA-BT). This is similar to (1.5) with the condition $\alpha_n = 1/L$ and

$$\theta_n = \frac{t_n - 1}{t_{n+1}}, \quad \text{where } t_{n+1} = \frac{1 + \sqrt{1 + 4t_n^2}}{2} \quad \text{and} \quad t_1 = 1. \tag{1.6}$$

Many proximal gradient methods usually use the assumption that the gradient is Lipschitz continuous and the step size is bounded below the Lipschitz constant. This is somehow not known in practice. For this reason, Bello Cruz and Nghia [25] proposed the linesearch rule by setting $\alpha_n = \sigma\theta^{m_n}$ and $m_n$ is the smallest nonnegative integer such that

$$\alpha_n \|\nabla f(k^{n+1}) - \nabla f(k^n)\| \le \delta \|k^{n+1} - k^n\|. \tag{1.7}$$

A new version of the forward–backward method (FISTA-CN) based on (1.7) is generated by the following:

$$x^n = k^n + \theta_n(k^n - k^{n-1}), \quad y^n = P_\Omega(x^n), \quad k^{n+1} = \mathrm{prox}_{\alpha_n g}(y^n - \alpha_n \nabla f(y^n)),$$

where the inertial parameter $\theta_n$ is defined by (1.6). Recently, Verma and Shukla [26] introduced a new accelerated proximal gradient algorithm (NAGA), which is defined by $k^0 = k^1 \in H$ and

$$\begin{aligned} x^n &= k^n + \theta_n(k^n - k^{n-1}), \\ y^n &= (1 - \alpha_n)x^n + \alpha_n \mathrm{prox}_{\alpha_n g}(x^n - \alpha_n \nabla f(x^n)), \\ k^{n+1} &= \mathrm{prox}_{\alpha_n g}(y^n - \alpha_n \nabla f(y^n)), \end{aligned}$$

where $\alpha_n \in (0, 2/L)$ and $\theta_n$ is defined by (1.6).

Motivated by previous works, in this work, we are interested to introduce a new inertial proximal algorithm for solving the convex MNPs and provide a weak convergence theorem for the proposed algorithm without the Lipschitz continuity condition on the gradient. We provide numerical experiments for our algorithm to solve image recovery problems and show the efficiency of the proposed algorithms when compared with FBS-CW [1], FISTA-BT [24], FISTA-CN [25], FBFS [17], and NAGA [26].

## 2 Main theorem

Now, we assume that $f : H \to \mathbb{R} \cup \{+\infty\}$ and $g : H \to \mathbb{R} \cup \{+\infty\}$ are proper, lower semicontinuous, and convex functions, $f$ is uniformly continuous on bounded sets, and $\nabla f$ is bounded on bounded sets. The following is our algorithm.

**Algorithm 2.1.** The inertial modified FBS (IMFBS) algorithm.

**Initialization:** Given $\sigma, \theta, \mu_1 > 0$, $\delta \in \left(0, \frac{1}{2}\right)$, and $\rho \in (0, 1)$.

**Iterative step:** Let $k^0 = k^1 \in H$ and calculate $k^{n+1}$ as follows:

**Step 1.** Compute the inertial step:

$$x^n = k^n + \theta_n(k^n - k^{n-1}),$$

where $(\theta_n)$ is a positive sequence.

**Step 2.** Compute the forward–backward step:

$$p^n = \operatorname{prox}_{\alpha_n g}(x^n - \alpha_n \nabla f(x^n)),$$

where $\alpha_n = \sigma\theta^{m_n}$ and $m_n$ is the smallest nonnegative number such that:

$$\alpha_n \|\nabla f(p^n) - \nabla f(x^n)\| \le \delta \|p^n - x^n\|. \tag{2.1}$$

**Step 3.** Compute the forward–backward step:

$$r^n = \operatorname{prox}_{\mu_n g}(p^n - \mu_n \nabla f(p^n)).$$

**Step 4.** Compute the $k^{n+1}$ step:

$$k^{n+1} = r^n + \mu_n(\nabla f(p^n) - \nabla f(r^n))$$

and update

$$\mu_{n+1} = \begin{cases} \min\left(\dfrac{\rho\|p^n - r^n\|}{\|\nabla f(p^n) - \nabla f(r^n)\|}, \mu_n\right) & \text{if } \|\nabla f(p^n) - \nabla f(r^n)\| \neq 0; \\ \mu_n & \text{otherwise}. \end{cases} \tag{2.2}$$

Set $n := n + 1$ and return to **Step 1.**

**Remark 2.2.**

(1) By [25], we know that the Linesearch (2.1) stops after finitely many steps.

(2) By (2.2), we see that the sequence $(\mu_n)$ is nonincreasing.

**Theorem 2.3.** *Suppose that $\alpha_n \ge \alpha$ for some $\alpha > 0$, $\theta_n \ge 0$, and $\sum_{n=1}^{\infty}\theta_n < +\infty$. Then, the sequence $(k^n)$ generated by Algorithm* 2.1 *converges weakly to a minimizer of $f + g$.*

**Proof.** Let $k_* \in \operatorname{argmin}(f + g)$. Following the definition of $r^n$, we have

$$p^n - r^n - \mu_n \nabla f(p^n) \in \mu_n \partial g(r^n). \tag{2.3}$$

By definition of $k^{n+1}$, we see that

$$\mu_n \nabla f(p^n) = k^{n+1} - r^n + \mu_n \nabla f(r^n). \tag{2.4}$$

From (2.3) and (2.4), we have

$$p^n - k^{n+1} - \mu_n \nabla f(r^n) \in \mu_n \partial g(r^n). \tag{2.5}$$

Since $k_* \in \operatorname{argmin}(f + g)$, we obtain $-\mu_n \nabla f(k_*) \in \mu_n \partial g(k_*)$. Thus, by relation (2.5) and the monotonicity of $\partial g$, we have

$$\langle p^n - k^{n+1} - \mu_n(\nabla f(r^n) - \nabla f(k_*)), r^n - k_* \rangle \ge 0.$$

This, together with the monotonicity of $\nabla f$, implies that

$$\langle p^n - k^{n+1}, r^n - k_* \rangle \ge 0.$$

Hence, we have

$$\langle p^n - k^{n+1}, r^n - k^{n+1} \rangle + \langle p^n - k^{n+1}, k^{n+1} - k_* \rangle \ge 0. \tag{2.6}$$

We know that $\|x \pm y\|^2 = \|x\|^2 \pm 2\langle x, y\rangle + \|y\|^2$. So by (2.6), we obtain

$$\frac{1}{2}[\|p^n - k^{n+1}\|^2 + \|k^{n+1} - r^n\|^2 - \|p^n - r^n\|^2] + \frac{1}{2}[\|p^n - k_*\|^2 - \|p^n - k^{n+1}\|^2 - \|k^{n+1} - k_*\|^2] \geq 0.$$

It implies that

$$\|k^{n+1} - k_*\|^2 \leq \|p^n - k_*\|^2 + \|k^{n+1} - r^n\|^2 - \|p^n - r^n\|^2. \tag{2.7}$$

By definition of $k^{n+1}$ and (2.2), we have

$$\|k^{n+1} - r^n\|^2 \leq \|r^n + \mu_n(\nabla f(p^n) - \nabla f(r^n)) - r^n\|^2 = \mu_n^2\|\nabla f(p^n) - \nabla f(r^n)\|^2. \tag{2.8}$$

Note that

$$\mu_{n+1} = \min\left(\frac{\rho\|p^n - r^n\|}{\|\nabla f(p^n) - \nabla f(r^n)\|}, \mu_n\right) \leq \frac{\rho\|p^n - r^n\|}{\|\nabla f(p^n) - \nabla f(r^n)\|}.$$

It follows that

$$\|\nabla f(p^n) - \nabla f(r^n)\| \leq \frac{\rho}{\mu_{n+1}}\|p^n - r^n\|. \tag{2.9}$$

Combining (2.8) and (2.9), we have

$$\|k^{n+1} - r^n\|^2 \leq \frac{\rho^2\mu_n^2}{\mu_{n+1}^2}\|p^n - r^n\|^2. \tag{2.10}$$

By definition of $p^n$, we have

$$\frac{x^n - p^n}{\alpha_n} - \nabla f(x^n) \in \partial g(p^n).$$

By the convexity of $g$, we obtain

$$g(k_*) - g(p^n) \geq \left\langle \frac{x^n - p^n}{\alpha_n} - \nabla f(x^n), k_* - p^n \right\rangle. \tag{2.11}$$

By the convexity of $f$, we see that

$$f(k_*) - f(x^n) \geq \langle \nabla f(x^n), k_* - x^n\rangle. \tag{2.12}$$

Combining (2.1), (2.11), and (2.12), we have

$$\begin{aligned}(f+g)(k_*) &\geq g(p^n) + f(x^n) + \left\langle \frac{x^n - p^n}{\alpha_n} - \nabla f(x^n), k_* - p^n \right\rangle + \langle \nabla f(x^n), k_* - x^n\rangle \\ &= g(p^n) + f(x^n) + \frac{1}{\alpha_n}\langle x^n - p^n, k_* - p^n\rangle + \langle \nabla f(x^n) - \nabla f(p^n), p^n - x^n\rangle + \langle \nabla f(p^n), p^n - x^n\rangle \\ &\geq g(p^n) + f(x^n) + \frac{1}{\alpha_n}\langle x^n - p^n, k_* - p^n\rangle - \|\nabla f(x^n) - \nabla f(p^n)\|\|p^n - x^n\| \\ &\quad + \langle \nabla f(p^n), p^n - x^n\rangle \\ &\geq g(p^n) + f(x^n) + \frac{1}{\alpha_n}\langle x^n - p^n, k_* - p^n\rangle - \frac{\delta}{\alpha_n}\|p^n - x^n\|^2 + \langle \nabla f(p^n), p^n - x^n\rangle.\end{aligned} \tag{2.13}$$

By (2.13) and the convexity of $f$, we obtain

$$\begin{aligned}\frac{1}{\alpha_n}\langle x^n - p^n, p^n - k_*\rangle &\geq g(p^n) + f(x^n) - (f+g)(k_*) - \frac{\delta}{\alpha_n}\|p^n - x^n\|^2 + f(p^n) - f(x^n) \\ &= (f+g)(p^n) - (f+g)(k_*) - \frac{\delta}{\alpha_n}\|p^n - x^n\|^2.\end{aligned} \tag{2.14}$$

We see that $\|x^n - k_*\|^2 = \|x^n - p^n\|^2 + 2\langle x^n - p^n, p^n - k_*\rangle + \|p^n - k_*\|^2$. By (2.14), we have

$$\|x^n - k_*\|^2 - \|x^n - p^n\|^2 - \|p^n - k_*\|^2 \geq 2\alpha_n[(f+g)(p^n) - (f+g)(k_*)] - 2\delta\|p^n - x^n\|^2.$$

It implies that

$$\|p^n - k_*\|^2 \le \|x^n - k_*\|^2 - (1-2\delta)\|x^n - p^n\|^2 - 2\alpha_n[(f+g)(p^n) - (f+g)(k_*)]. \tag{2.15}$$

Hence, from (2.7), (2.10), and (2.15), we obtain

$$\begin{aligned}\|k^{n+1} - k_*\|^2 \le{}& \|x^n - k_*\|^2 - (1-2\delta)\|x^n - p^n\|^2 - 2\alpha_n[(f+g)(p^n) - (f+g)(k_*)]\\ &- \left(1 - \frac{\rho^2\mu_n^2}{\mu_{n+1}^2}\right)\|p^n - r^n\|^2.\end{aligned} \tag{2.16}$$

Now, we will show that $(k^n)$ is bounded. From (2.16) and by definition of $(x^n)$, we have

$$\|k^{n+1} - k_*\| \le \|x^n - k_*\| = \|k^n + \theta_n(k^n - k^{n-1}) - k_*\| \le \|k^n - k_*\| + \theta_n(\|k^n - k_*\| + \|k^{n-1} - k_*\|).$$

This shows that

$$\|k^{n+1} - k_*\| \le (1+\theta_n)\|k^n - k_*\| + \theta_n\|k^{n-1} - k_*\|.$$

By Lemma 5 in [27], we conclude that

$$\|k^{n+1} - k_*\| \le K \cdot \prod_{j=1}^{n}(1 + 2\theta_j),$$

where $K = \max\{\|k^1 - k_*\|, \|k^2 - k_*\|\}$. Since $\sum_{n=1}^{\infty}\theta_n < +\infty$, we have $(k^n)$, which is bounded. From (2.16), we have

$$\begin{aligned}\|k^{n+1} - k_*\|^2 \le{}& \|k^n + \theta_n(k^n - k^{n-1}) - k_*\|^2 - (1-2\delta)\|x^n - p^n\|^2 - 2\alpha_n[(f+g)(p^n) - (f+g)(k_*)]\\ &- \left(1 - \frac{\rho^2\mu_n^2}{\mu_{n+1}^2}\right)\|p^n - r^n\|^2\\ ={}& \|k^n - k_*\|^2 + 2\theta_n\|k^n - k_*\|\|k^n - k^{n-1}\| + \theta_n^2\|k^n - k^{n-1}\|^2 - (1-2\delta)\|x^n - p^n\|^2\\ &- 2\alpha_n[(f+g)(p^n) - (f+g)(k_*)] - \left(1 - \frac{\rho^2\mu_n^2}{\mu_{n+1}^2}\right)\|p^n - r^n\|^2.\end{aligned} \tag{2.17}$$

Since $\lim_{n\to\infty}\theta_n\|k^n - k^{n-1}\| = 0$, $\lim_{n\to\infty}\|k^n - k_*\|$ exists, and $1 - 2\delta > 0$, we have

$$\lim_{n\to\infty}\|x^n - p^n\| = 0.$$

By definition of $x^n$, we have $\lim_{n\to\infty}\|x^n - k^n\| = 0$. Then,

$$\|p^n - k^n\| \le \|x^n - p^n\| + \|x^n - k^n\| \to 0 \quad \text{as } n \to \infty.$$

Since $\lim_{n\to\infty}\left(1 - \frac{\mu_n^2\rho^2}{\mu_{n+1}^2}\right) = 1 - \rho^2 > 0$, we have $\lim_{n\to\infty}\|p^n - r^n\| = 0$. So, we have

$$\|r^n - k^n\| \le \|p^n - r^n\| + \|p^n - k^n\| \to 0 \quad \text{as } n \to \infty.$$

Since the sequence $(k^n)$ is bounded, assume that $k^\infty$ is a weak limit point of $(k^n)$, i.e., there is a subsequence $(k^{n_i})$ of $(k^n)$ such that $k^{n_i} \rightharpoonup k^\infty$. Since $\lim_{i\to\infty}\|r^{n_i} - k^{n_i}\| = 0$, we also obtain $r^{n_i} \rightharpoonup k^\infty$ as $i \to \infty$. Since $(p^{n_i})$ is bounded, $\lim_{i\to\infty}\|p^{n_i} - r^{n_i}\| = 0$, and $\nabla f$ is uniformly continuous on $H$, we have

$$\lim_{i\to\infty}\|\nabla f(p^{n_i}) - \nabla f(r^{n_i})\| = 0.$$

From (1.3), we obtain

$$\frac{p^{n_i} - r^{n_i}}{\alpha_{n_i}} - \nabla f(p^{n_i}) = \frac{p^{n_i} - \mathrm{prox}_{\alpha_{n_i}g}(p^{n_i} - \alpha_{n_i}\nabla f(p^{n_i})) - \alpha_{n_i}\nabla f(p^{n_i})}{\alpha_{n_i}} \in \partial g\big(p^{n_i} - \alpha_{n_i}\nabla f(p^{n_i})\big).$$

It follows that

$$\frac{p^{n_i} - r^{n_i}}{\alpha_{n_i}} + \nabla f(r^{n_i}) - \nabla f(p^{n_i}) \in \nabla f(r^{n_i}) + \partial g(r^{n_i}) \subseteq \partial(f+g)(r^{n_i}).$$

By passing $i \to \infty$ and using Fact 2.2 in [25], we have $0 \in \nabla f(k^\infty) + \partial g(k^\infty)$. Thus, $k^\infty \in \operatorname{argmin}(f+g)$. Hence, by Theorem 5.5 in [28], we can conclude that $(k^n)$ converges weakly to a point in $\operatorname{argmin}(f+g)$. We thus complete the proof. □

# 3 Numerical experiments

In this section, we apply Algorithm 2.1 to solve the image restoration problem and compare the efficiency of FBS-CW [1], FISTA-BT [24], FISTA-CN [25], FBFS [17], and NAGA [26]. The numerical experiments are performed by Matlab 2020b on a 64-bit MacBook Pro Chip Apple M1 and 8 GB of RAM.

The image restoration problem can be modeled as follows:

$$b = Ak + w, \tag{3.1}$$

where $b \in \mathbb{R}^{m\times 1}$ is the observed image, $A \in \mathbb{R}^{m\times n}$ is the blurring matrix, $k \in \mathbb{R}^{n\times 1}$ is an original image, and $w$ is additive noise. To solve problem (3.1), we aim to approximate the original image by transforming (3.1) to the following LASSO problem [29]:

$$\min_k \left(\frac{1}{2}\|b - Ak\|_2^2 + \lambda\|k\|_1\right), \tag{3.2}$$

where $\|\cdot\|_1$ is $\ell_1$-norm. In general, (3.2) can be formulated in a general form by estimating the minimizer of the sum of two functions when $f(k) = \frac{1}{2}\|b - Ak\|_2^2$ and $g(k) = \lambda\|k\|_1$.

To evaluate the quality of the restored images, we use the peak signal-to-noise ratio (PSNR) [30] and the structural similarity index (SSIM) [31], which are defined as follows:

$$\mathrm{PSNR} = 20\log\frac{\|k\|_F}{\|k - k^r\|_F} \tag{3.3}$$

and

$$\mathrm{SSIM} = \frac{(2u_k u_{k^r} + c_1)(2\sigma_{kk^r} + c_2)}{(u_k^2 + u_{k^r}^2 + c_1)(\sigma_x^2 + \sigma_{k^r}^2 + c_2)}, \tag{3.4}$$

where $k$ is the original image, $k^r$ is the restored image, $u_k$ and $u_{k^r}$ are the mean values of the original image $k$ and restored image $k^r$, respectively, $\sigma_k^2$ and $\sigma_{k^r}^2$ are the variances, $\sigma_{kk^r}^2$ is the covariance of two images, $c_1 = (K_1L)^2$ and $c_2 = (K_2L)^2$ with $K_1 = 0.01$ and $K_2 = 0.03$, and $L$ is the dynamic range of pixel values. SSIM ranges from 0 to 1, and 1 means perfect recovery.

All parameters are chosen as in Table 1. The initial point $k^0 = k^1$ are vectors of ones with the size of the original images for all algorithms. The parameter $\theta_n$ of FISTA-BT, FISTA-CN, and NAGA is defined as (1.6). We also set $\theta_n$ in Algorithm 2.1 (IMFBS) by

**Table 1:** Chosen parameters of each algorithm

| **Algorithms** | **Chosen parameters** | | | | | |
|---|---|---|---|---|---|---|
| | $t_1 = 1$ | $\alpha_n = 1/2\|A\|^2$ | $\lambda_n = 0.5$ | $\delta = \theta = 0.4$ | $\sigma = 0.2$ | $\rho = \mu_1 = 0.4$ |
| FBS-CW | | √ | √ | | | |
| FISTA-BT | √ | √ | | | | |
| FISTA-CN | √ | | | √ | √ | |
| NAGA | √ | √ | | | | |
| FBFS | | √ | | | | |
| IMFBS | √ | | | √ | √ | √ |

(Fig(A)) (BM-1.1) (BM-1.2) (BM-1.3)

**Figure 1:** The original image size 448 × 298 (Fig(A)) and the deblurred RGB images by out-of-focus blur matrices with radius 6 (BM-1.1), Gaussian blur with standard deviation 7 of the filter size [5 × 5] (BM-1.2), and the deblurred images by motion blur specified with the motion length of 11 pixels and motion orientation 23 (BM-1.3), respectively.

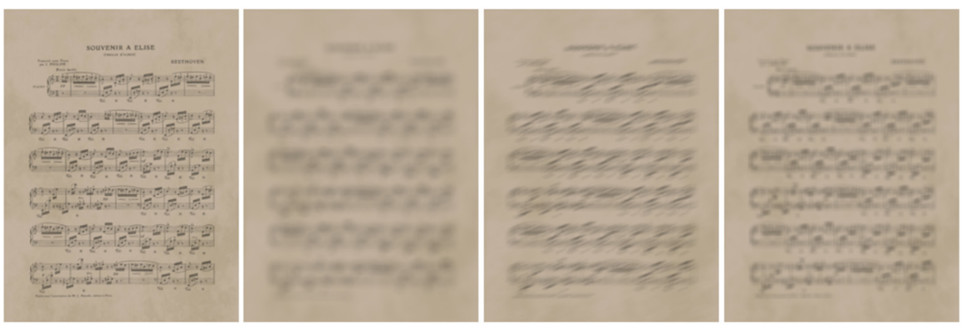

(Fig(B)) (BM-2.1) (BM-2.2) (BM-2.3)

**Figure 2:** The original image size 240 × 320 (Fig(A)) and the deblurred RGB image by out-of-focus blur matrices with radius 6 (BM-1.1), Gaussian blur with standard deviation 7 of the filter size [5 × 5] (BM-2.2), and the deblurred image by motion blur specified with the motion length of 11 pixels and motion orientation 23 (BM-2.3), respectively.

**Table 2:** The results of deblurred images for each algorithm

| **Fig(A)** | ***M*** | **Algorithms** | **Blurred type** | | | | | |
|---|---|---|---|---|---|---|---|---|
| | | | **BM-1.1** | | **BM-1.2** | | **BM-1.3** | |
| | | | **PSNR** | **SSIM** | **PSNR** | **SSIM** | **PSNR** | **SSIM** |
| The original image size 448 × 298 | 500 | FBS-CW | 25.8764 | 0.7715 | 29.0112 | 0.8899 | 31.2942 | 0.9242 |
| | | FISTA-BT | 35.5477 | 0.9446 | 38.3302 | 0.9621 | 40.5405 | 0.9835 |
| | | FISTA-CN | 36.5491 | 0.9543 | 39.5388 | 0.9705 | 41.8671 | 0.9871 |
| | | NAGA | 36.2057 | 0.9514 | 39.1270 | 0.9678 | 41.4341 | 0.9859 |
| | | FBFS | 24.2054 | 0.7072 | 27.5600 | 0.8583 | 29.8552 | 0.8996 |
| | | IMFBS | 38.7966 | 0.9702 | 41.6765 | 0.9816 | 44.6781 | 0.9930 |
| | 1,000 | FBS-CW | 26.1910 | 0.7837 | 29.2922 | 0.8957 | 31.5644 | 0.9286 |
| | | FISTA-BT | 37.0305 | 0.9586 | 39.6679 | 0.9715 | 41.7964 | 0.9883 |
| | | FISTA-CN | 38.1887 | 0.9664 | 40.9419 | 0.9780 | 43.1783 | 0.9911 |
| | | NAGA | 37.7800 | 0.9641 | 40.5485 | 0.9759 | 42.6821 | 0.9901 |
| | | FBFS | 24.6732 | 0.7225 | 27.8260 | 0.8662 | 30.1126 | 0.9053 |
| | | IMFBS | 40.5491 | 0.9782 | 43.2354 | 0.9868 | 45.9856 | 0.9950 |
| | 1,500 | FBS-CW | 26.4418 | 0.7923 | 29.5205 | 0.8996 | 31.7869 | 0.9318 |
| | | FISTA-BT | 38.0757 | 0.9664 | 40.6216 | 0.9765 | 42.6318 | 0.9906 |
| | | FISTA-CN | 39.2981 | 0.9726 | 41.9730 | 0.9833 | 44.0774 | 0.9330 |
| | | NAGA | 38.8771 | 0.9708 | 41.5473 | 0.9813 | 43.5755 | 0.9923 |
| | | FBFS | 24.8915 | 0.7331 | 28.0377 | 0.8717 | 30.3250 | 0.9094 |
| | | IMFBS | 41.7181 | 0.9828 | 44.4942 | 0.9901 | 47.3108 | 0.9964 |

**Table 3:** The results of deblurred images for each algorithm

| Fig(B) | *M* | Algorithms | Blurred type | | | | | |
|---|---|---|---|---|---|---|---|---|
| | | | BM-2.1 | | BM-2.2 | | BM-2.3 | |
| | | | PSNR | SSIM | PSNR | SSIM | PSNR | SSIM |
| The original image size 240 × 320 | 500 | FBS-CW | 28.1063 | 0.8764 | 33.3164 | 0.9479 | 32.8894 | 0.9503 |
| | | FISTA-BT | 38.4144 | 0.9733 | 42.9090 | 0.9888 | 42.9989 | 0.9911 |
| | | FISTA-CN | 39.3158 | 0.9779 | 43.9720 | 0.9910 | 44.3774 | 0.9932 |
| | | NAGA | 39.0548 | 0.9767 | 43.6322 | 0.9904 | 43.9016 | 0.9926 |
| | | FBFS | 26.7863 | 0.8427 | 31.5921 | 0.9344 | 31.3430 | 0.9354 |
| | | IMFBS | 41.2504 | 0.9843 | 46.2374 | 0.9945 | 46.6263 | 0.9958 |
| | 1,000 | FBS-CW | 28.3151 | 0.8818 | 33.5886 | 0.9507 | 33.1323 | 0.9530 |
| | | FISTA-BT | 39.1638 | 0.9772 | 43.9748 | 0.9912 | 44.0517 | 0.9931 |
| | | FISTA-CN | 40.1671 | 0.9813 | 45.1091 | 0.9929 | 45.4008 | 0.9948 |
| | | NAGA | 39.9064 | 0.9804 | 44.7171 | 0.9923 | 45.1169 | 0.9945 |
| | | FBFS | 26.9618 | 0.8486 | 31.8549 | 0.9378 | 31.5693 | 0.9388 |
| | | IMFBS | 42.2498 | 0.9874 | 47.3408 | 0.9957 | 47.6728 | 0.9968 |
| | 1,500 | FBS-CW | 28.5033 | 0.8862 | 33.8154 | 0.9526 | 33.3404 | 0.9549 |
| | | FISTA-BT | 39.7800 | 0.9800 | 44.7409 | 0.9925 | 44.9116 | 0.9943 |
| | | FISTA-CN | 40.8390 | 0.9836 | 45.9122 | 0.9941 | 46.2742 | 0.9957 |
| | | NAGA | 40.4829 | 0.9825 | 45.5109 | 0.9936 | 45.8330 | 0.9953 |
| | | FBFS | 27.1200 | 0.8534 | 32.0793 | 0.9402 | 31.7652 | 0.9412 |
| | | IMFBS | 43.0213 | 0.9891 | 48.0766 | 0.9963 | 48.6282 | 0.9974 |

(FBS-CW) (FISTA-BT) (FISTA-CN) (NAGA) (FBFS) (IMFBS)

**Figure 3:** The restored images by BM-1.1 for FBS-CW (PSNR:26.07923, SSIM:0.7923), FISTA-BT (PSNR:38.9664, SSIM:0.9664), FISTA-CN (PSNR:39.2981, SSIM:0.9726), NAGA (PSNR:38.8771 SSIM:0.9708), FBFS (PSNR:24.8915 SSIM:0.7331), and IMFBS (PSNR:41.7181, SSIM:0.9828), respectively.

(FBS-CW) (FISTA-BT) (FISTA-CN) (NAGA) (FBFS) (IMFBS)

**Figure 4:** The restored images by BM-1.2 for FBS-CW (PSNR:29.5205, SSIM:0.8996), FISTA-BT (PSNR:40.6212, SSIM:0.9765), FISTA-CN (PSNR:41.9730, SSIM:0.9833), NAGA (PSNR:41.5473, SSIM:0.9813), FBFS (PSNR:28.0377, SSIM:0.8717), and IMFBS (PSNR:44.4942, SSIM:0.9901), respectively.

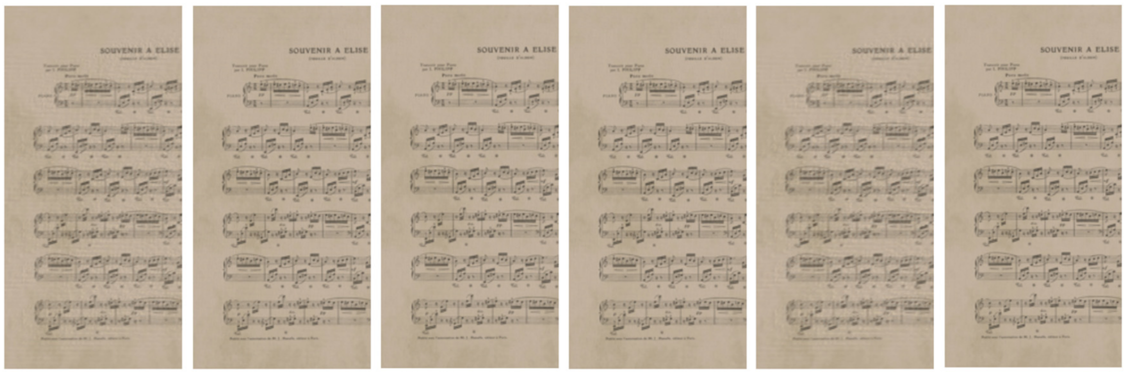


(FBS-CW) (FISTA-BT) (FISTA-CN) (NAGA) (FBFS) (IMFBS)

**Figure 5:** The restored images by BM-2.3 for FBS-CW (PSNR:33.3404, SSIM:0.9549), FISTA-BT (PSNR:44.9116, SSIM:0.9943), FISTA-CN (PSNR:46.2742, SSIM:0.9957), NAGA (PSNR:45.8330, SSIM:0.9953), FBFS (PSNR:31.7652, SSIM:0.9412), and IMFBS (PSNR:48.6282, SSIM:0.9974), respectively.

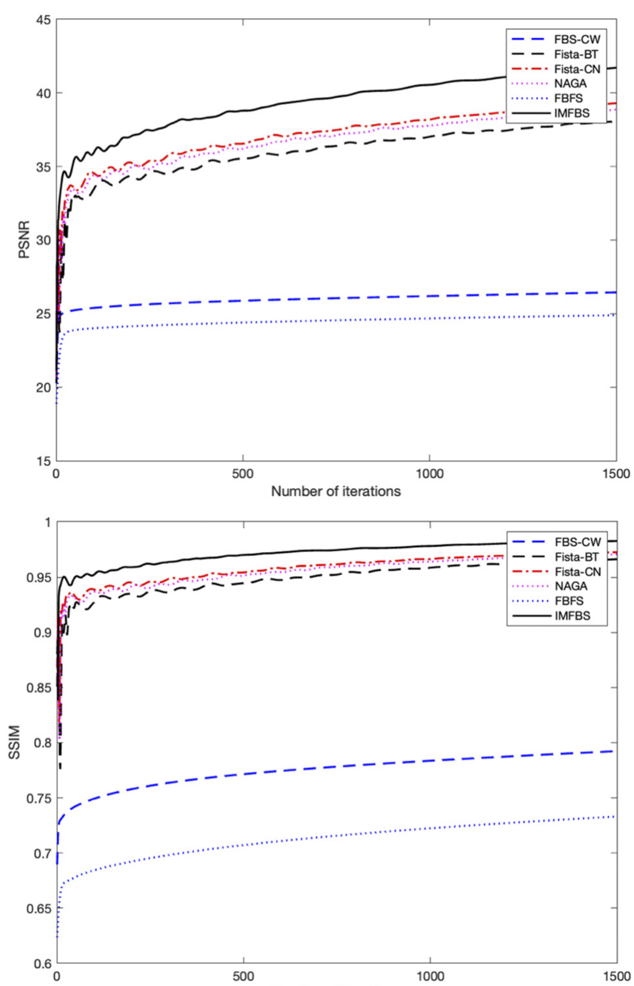


**Figure 6:** Graphs of PSNR and SSIM for FIG(A) by out of focusing, respectively.

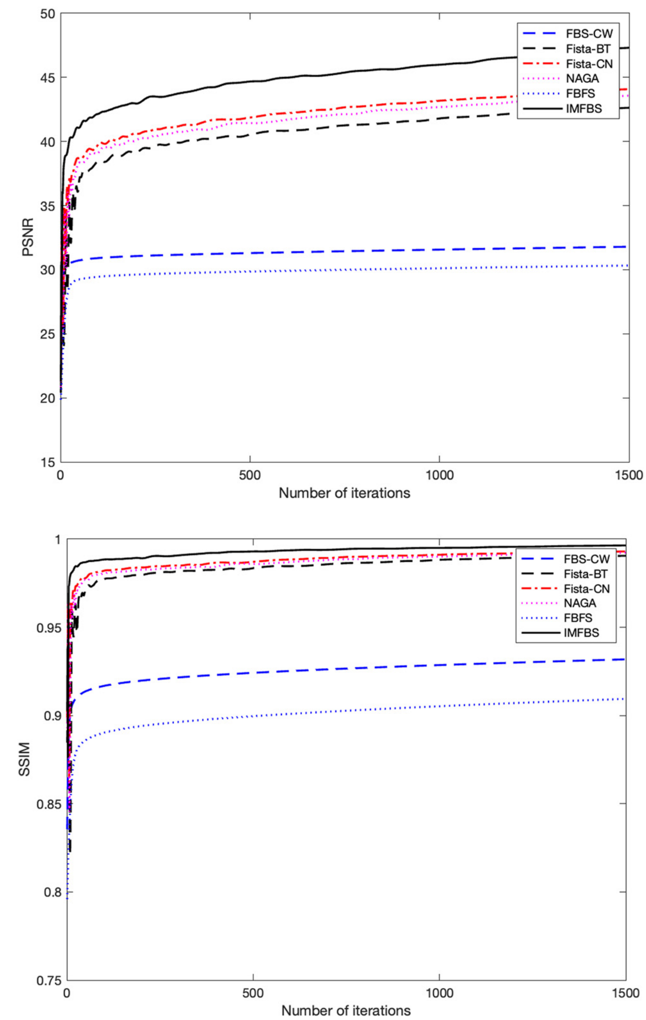


**Figure 7:** Graphs of PSNR and SSIM for FIG(A) by Gaussian blur matrices, respectively.

$$\theta_n = \begin{cases} \dfrac{t_n - 1}{t_{n+1}} \quad \text{where } t_{n+1} = \dfrac{1 + \sqrt{1 + 4t_n^2}}{2}, & \text{if } 1 \le n \le M; \\ \dfrac{1}{n^2}, & \text{otherwise}. \end{cases}$$

The original images and three different blurring matrices types for the original images of sizes $448 \times 298$ and $240 \times 320$ are shown in Figures 1 and 2, respectively.

The results of the deblurred images with $M$ iterations for each algorithm are shown in Tables 2 and 3. We provide some experiments of recovered images of Fig(A) for two cases and one case for Fig(B) to illustrate the convergence behavior of all algorithms in Figures 3–5.

In Figures 6–8, we plot the number of iterations versus the PSNR [30] and the SSIM [31].

## 4 Conclusion

In this work, we have introduced a new inertial proximal gradient algorithm for solving the convex MNPs and have proved a weak convergence theorem without the Lipschitz continuity conditions on the gradient

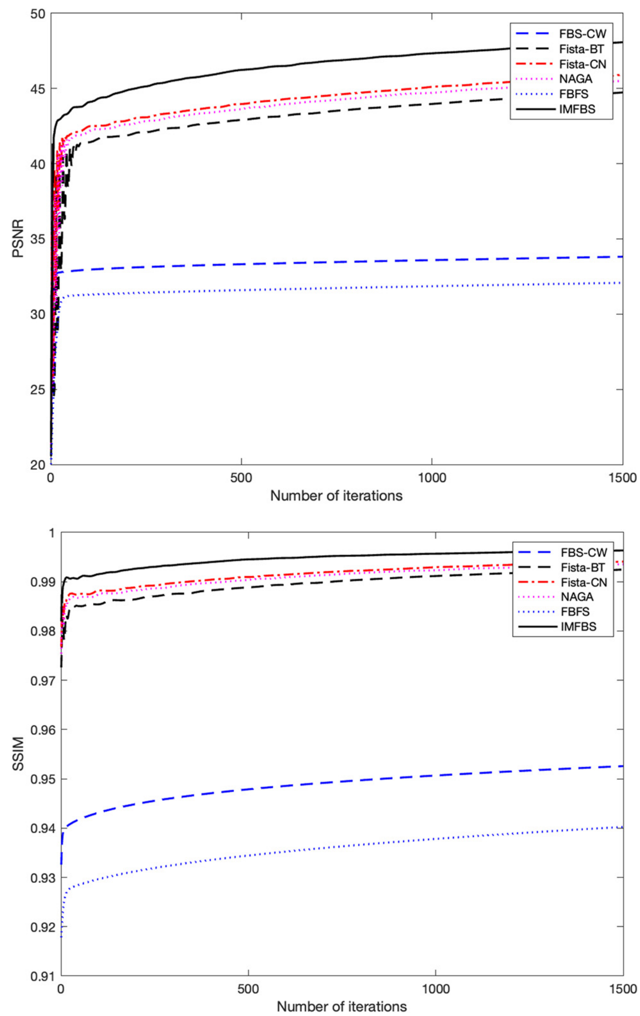


**Figure 8:** Graphs of PSNR and SSIM for Fig(B) by motion blurring, respectively.

of functions. We provided some numerical experiments and applied our algorithm to the image recovery problem. We also compared our algorithm with FBS-CW [1], FISTA-BT [24], FISTA-CN [25], FBFS [17], and NAGA [26]. It was shown that our algorithm has better efficiency than other algorithms in terms of PSNR and SSIM for all blurred types.

**Acknowledgement:** The authors sincerely thank the anonymous reviewers for their careful reading, constructive comments, and suggestions for some related references that improved the manuscript substantially.

**Funding information**: This work was supported by the National Research Council of Thailand under grant no. N41A640094 and the Thailand Science Research and Innovation Fund and the University of Phayao under the project FF66-UoE.

**Author contributions**: The authors conceived the study, participated in its design and coordination, drafted the manuscript, participated in the sequence alignment, and read and approved the final manuscript.

**Conflict of interest**: The authors declare that they have no competing interests.

**Data availability statement**: Data sharing is not applicable to this article as no datasets were generated or analyzed during this study.

# References


[1] P. L. Combettes and V. R. Wajs, *Signal recovery by proximal forward–backward splitting*, Multiscale Model. Simul. **4** (2005), 1168–1200, DOI: https://doi.org/10.1137/050626090.

[2] P. L. Lions and B. Mercier, *Splitting algorithms for the sum of two nonlinear operators*, SIAM J. Numer. Anal. **16** (1979), 964–979, DOI: https://doi.org/10.1137/0716071.

[3] S. Khatoon, W. Cholamjiak, and I. Uddin, *A modified proximal point algorithm involving nearly asymptotically quasi-nonexpansive mappings*, J. Inequal. Appl. **2021** (2021), 1–20, DOI: https://doi.org/10.1186/s13660-021-02618-7.

[4] S. Khatoon, I. Uddin, and M. Basarir, *A modified proximal point algorithm for a nearly asymptotically quasi-nonexpansive mapping with an application*, Comput. Appl. Math. **40** (2021), 1–19, DOI: https://doi.org/10.1007/s40314-021-01646-9.

[5] C. Khunpanuk, C. Garodia, I. Uddin, and N. Pakkaranang, *On a proximal point algorithm for solving common fixed point problems and convex minimization problems in Geodesic spaces with positive curvature*, AIMS Math. **7** (2022), 9509–9523, DOI: https://doi.org/10.3934/math.2022529.

[6] C. Garodia, I. Uddin, and D. Baleanu, *On constrained minimization, variational inequality and split feasibility problem via new iteration scheme in Banach spaces*, Bull. Iran. Math. Soc. **48** (2022), 1493–1512, DOI: https://doi.org/10.1007/s41980-021-00596-6.

[7] T. Kajimura and Y. Kimura, *The proximal point algorithm in complete geodesic spaces with negative curvature*, Adv. Theory Nonlinear Anal. Appl. **3** (2019), 192–200, DOI: https://doi.org/10.31197/atnaa.573972.

[8] M. A. Hajji, *Forward-backward alternating parallel shooting method for multi-layer boundary value problems*, Adv. Theory Nonlinear Anal. Appl. **4** (2020), 432–442, DOI: https://doi.org/10.31197/atnaa.753561.

[9] A. N. Iusem, B. F. Svaiter, and M. Teboulle, *Entropy-like proximal methods in convex programming*, Math. Oper. Res. **19** (1994), 790–814, DOI: https://doi.org/10.1287/moor.19.4.790.

[10] J. C. Dunn, *Convexity, monotonicity, and gradient processes in Hilbert space*, J. Math. Anal. Appl. **53** (1976), 145–158, DOI: https://doi.org/10.1016/0022-247X(76)90152-9.

[11] C. Wang and N. Xiu, *Convergence of the gradient projection method for generalized convex minimization*, Comput. Optim. Appl. **16** (2000), 111–120, DOI: https://doi.org/10.1023/A:1008714607737.

[12] H. K. Xu, *Averaged mappings and the gradient-projection algorithm*, J. Optim. Theory Appl. **150** (2011), 360–378, DOI: https://doi.org/10.1007/s10957-011-9837-z.

[13] K. Kankam, N. Pholasa, and P. Cholamjiak, *On convergence and complexity of the modified forward-Řbackward method involving new linesearches for convex minimization*. Math. Methods Appl. Sci. **42** (2019), 1352–1362, DOI: https://doi.org/10.1002/mma.5420.

[14] S. Suantai, M. A. Noor, K. Kankam, and P. Cholamjiak, *Novel forward–backward algorithms for optimization and applications to compressive sensing and image inpainting*, Adv. Difference Equ. **2021** (2021), 1–22, DOI: https://doi.org/10.1186/s13662-021-03422-9.

[15] K. Kankam, N. Pholasa, and P. Cholamjiak, *Hybrid forward–backward algorithms using linesearch rule for minimization problem*, Thai J. Math. **17** (2019), 607–625.

[16] K. Kankam and P. Cholamjiak, *Strong convergence of the forward–backward splitting algorithms via linesearches in Hilbert spaces*, Appl. Anal. **2021** (2021), 1–20, DOI: https://doi.org/10.1080/00036811.2021.1986021.

[17] P. Tseng, *A modified forward–backward splitting method for maximal monotone mappings*, SIAM J. Control Optim. **38** (2000), 431–446, DOI: https://doi.org/10.1137/S0363012998338806.

[18] H. Attouch and J. Peypouquet, *The rate of convergence of Nesterov's accelerated forward–backward method is actually faster than* $1/k^2$, SIAM J. Control Optim. **26** (2016), 1824–1834, DOI: https://doi.org/10.1137/15M1046095.

[19] A. Moudafi and M. Oliny, *Convergence of a splitting inertial proximal method for monotone operators*, J. Comput. Appl. Math. **155** (2003), 447–454, DOI: https://doi.org/10.1016/S0377-0427(02)00906-8.

[20] Y. E. Nesterov, *A method for solving the convex programming problem with convergence rate* $O(1/k^2)$, Dokl. Akad. Nauk SSR. **269** (1983), 543–547.

[21] B. T. Polyak, *Some methods of speeding up the convergence of iteration methods*, USSR Comput. Math. Math. Phys. **4** (1964), 1–17, DOI: https://doi.org/10.1016/0041-5553(64)90137-5.

[22] F. Akutsah, A. A. Mebawondu, G. C. Ugwunnadi, and O. K. Narain, *Inertial extrapolation method with regularization for solving monotone bilevel variation inequalities and fixed point problems*, J. Nonlinear Funct. Anal. **2022** (2022), 5, DOI: https://doi.org/10.23952/jnfa.2022.5.

[23] L. Liu, S. Y. Cho, and J. C. Yao, *Convergence analysis of an inertial Tseng's extragradient algorithm for solving pseudo-monotone variational inequalities and applications*, J. Nonlinear Var. Anal. **5** (2021), 627–644.

[24] A. Beck and M. Teboulle, *A fast iterative shrinkage-thresholding algorithm for linear inverse problems*, SIAM J. Imaging Sci. **2** (2009), 183–202, DOI: https://doi.org/10.1137/080716542.

[25] J. Y. Bello Cruz and T. T. Nghia, *On the convergence of the forward–backward splitting method with linesearches*, Optim. Methods Softw. **31** (2016), 1209–1238, DOI: https://doi.org/10.1080/10556788.2016.1214959.

[26] M. Verma and K. K. Shukla, *A new accelerated proximal gradient technique for regularized multitask learning framework*, Pattern Recognit. Lett. **95** (2017), 98–103, DOI: https://doi.org/10.1016/j.patrec.2017.06.013.

[27] A. Hanjing and S. Suantai, *A fast image restoration algorithm based on a fixed point and optimization method*, Mathematics, **8** (2020), 378, DOI: https://doi.org/10.3390/math8030378.

[28] H. H. Bauschke and P. L. Combettes, *Convex Analysis and Monotone Operator Theory in Hilbert Spaces*, Springer, New York, 2011.

[29] R. Tibshirani, *Regression shrinkage and selection via the lasso*, J. R. Stat. Soc. Series B. Stat. Methodol. **58** (1996), 267–288, DOI: https://doi.org/10.1111/j.2517-6161.1996.tb02080.x.

[30] K. H. Thung and P. Raveendran, A survey of image quality measures. In *2009 International Conference for Technical Postgraduates* (*TECHPOS*), IEEE; 2009, December. p. 1–4.

[31] Z. Wang, A. C. Bovik, and E. P. Simoncelli, *Image quality assessment: from error visibility to structural similarity*, IEEE Trans. Image Process. **13** (2004), 600–612, DOI: https://doi.org/10.1109/TIP.2003.819861.